Flight Test Data Validation of Dual-Frequency GPS Measurement Error Characteristics

Tang, H. Walter, T. Blanch, J. Enge, P. *Stanford University*
Chan, F-C. *Illinois Institute of Technology*

Abstract

With the launch of the GPS-IIF satellites, the new civil navigation signals at L5 (1176.45 MHz) will become available to the GNSS community. One of the most significant benefits introduced by this new signal is that the dual-frequency measurement combination of L5 and the existing L1 C/A signals will eliminate the largest GPS measurement error - the ionosphere delay affecting the L1-only signal. The ionosphere delay will be removed by forming an Iono-free GPS code measurement combination with the dual-frequency signal. Thus, the performances of many GNSS navigation applications, such as the accuracy and integrity metrics in civil aviation, will be dramatically improved.

The dual-frequency code measurement combination process suppresses the ionosphere delay; however, it is a double-edged sword, as the combination also increases the contributions of multi-path and receiver noise errors on the GPS measurements. Therefore, carrier smoothing is applied to alleviate the negative impact of these errors. In this paper, the effects of these errors are investigated using the flight test GPS measurement data obtained from FAA flight trials conducted at Memphis International Airport. This data uses the currently available dual frequency data based upon L1 C/A and L2 P(Y) semi-codeless signals (since the L5 signal is not available yet, the L2 signal is used as a substitute). This paper also analyzes the effectiveness of the carrier smoothing process for airborne GPS code measurements, in mitigating the increased noise due to the Iono-free measurement combination. The resulting ranging signal qualities of the dual frequency measurements are compared against the qualities of the WAAS-corrected L1-only measurements.

Introduction

The ionosphere is a layer of atmosphere distributed from approximately 50km to 1000km above the earth ground. This layer of atmosphere is filled of free electrons and ions, the peak density of which resides in the height range from 250km to 400km. For the transmission of radio-frequency signals (GPS signals for instance), the electron density along the radio-frequency signal propagation path has effects on the signal refractive index:

$$n_g \approx 1 + \frac{40.3 n_e}{f^2}$$

Equation 1: Group refractive index

where, n_g is the group refractive index, n_e is the electron density and f is the signal frequency. Thus, the group delay of transmitting signals in the ionosphere can be calculated with [1]:

$$I_\rho = c \cdot \Delta\tau = c \cdot \frac{1}{c} \int_{SV}^{Rcvr} [n_g(l) - 1] dl$$

$$= c \cdot \frac{1}{c} \int_{SV}^{Rcvr} \frac{40.3 n_e(l)}{f^2} dl$$

$$= \frac{40.3 TEC}{f^2}$$

Equation 2: Group delay caused by ionosphere

where TEC (Total Electron Content) is the number of electrons in a tube with unit area cross section along the signal path from the satellite to the receiver.

The unknown ionosphere delay is a major error source for GPS signals. Therefore several methods have been developed to mitigate its effects: The most common implementation is to apply the Klobuchar model [2]. For users within the WAAS service volume it is possible to eliminate most of the ionosphere delays by

receiving and decoding the WAAS correction messages, and the residual error is much smaller than applying the Klobuchar model, but it is only available within the WAAS service volume (typically North America). The most accurate approach, which emerges with the up-coming second frequency of GPS civil signal – L5, is utilizing the dual-frequency measurement combination of L1 and L5, and this method will be available to users all over the world with the under-going GPS modernization.

Since the ionosphere delay of GPS signals is directly correlated with signal transmitting frequencies (shown in Equation 2), when signals with two different frequencies are transmitted simultaneously from a satellite to the GPS receiver, the receiver will be able to accurately calculate the ionosphere delay using this signal combination. The exact ionosphere delay is calculated with:

L1 signal: $$I_{L1} = \frac{{f_{L2}}^2}{{f_{L1}}^2 - {f_{L2}}^2}(\rho_{L2} - \rho_{L1})$$

L2 signal: $$I_{L2} = \frac{{f_{L1}}^2}{{f_{L1}}^2 - {f_{L2}}^2}(\rho_{L2} - \rho_{L1})$$

Equation 3: Ionosphere delay for L1 & L2 signals

and the dual-frequency iono-free measurement combination is:

$$\rho_{IF} = \frac{{f_{L1}}^2}{{f_{L1}}^2 - {f_{L2}}^2}\rho_{L1} - \frac{{f_{L2}}^2}{{f_{L1}}^2 - {f_{L2}}^2}\rho_{L2}$$

Equation 4: Dual-frequency measurement combination

Along with the advantage of removing the ionosphere delay, the dual-frequency measurement combination also significantly increases the signal multipath error and receiver noise. The increase of the noise distribution standard deviation may be as much as 3 times of single-frequency signals (the noises on L1 and L2 signals are regarded as equal):

$$\begin{aligned}\mathrm{var}(\varepsilon_{IF}) &= [\frac{{f_{L1}}^2}{{f_{L1}}^2 - {f_{L2}}^2}]\mathrm{var}(\varepsilon_{L1}) \\ &\quad -[\frac{{f_{L2}}^2}{{f_{L1}}^2 - {f_{L2}}^2}]^2\,\mathrm{var}(\varepsilon_{L2}) \\ &\approx 9\,\mathrm{var}(\varepsilon_{L1})\end{aligned}$$

Equation 5: Dual-frequency measurement multipath error and receiver noise variance

Carrier smoothing has been developed to reduce the GPS code measurement noise. In this paper, we will process the GPS measurement data obtained from one FAA flight test and generate the dual-frequency GPS measurements along with the L1-only single-frequency measurement. The airborne receiver clock error and dual-frequency measurement multipath errors and receiver noises will be inspected to help us better understand the dual-frequency measurement error characteristics in aviation applications and also benefit the GPS navigation integrity model development applied in civil aviations.

FAA Flight Test

The flight test GPS data was collected by the Federal Aviation Administration on the morning of September 19th, 2006, at Memphis International Airport, TN. The test aircraft is the FAA N47 Flying Laboratory (Figure 1), a dual-engine jet. The GPS receiver onboard of the aircraft is a Novatel receiver with WAAS capabilities. The flight test was started after the test aircraft took off and climbed onto a predefined altitude (~850m). Then a total of 8 test approaches were performed by that aircraft, in each the test aircraft made a descendant down to about 70m above the ground. After each approach finished (except the last one), the airplane climbed up again to 850m height,

Fig 1: FAA N47 Flying Lab

maintained the altitude for 4 minutes to 10 minutes and started the next test approach. Upon the finish of the final approach, the aircraft started the landing procedure and returned to the ground (Figure 2).

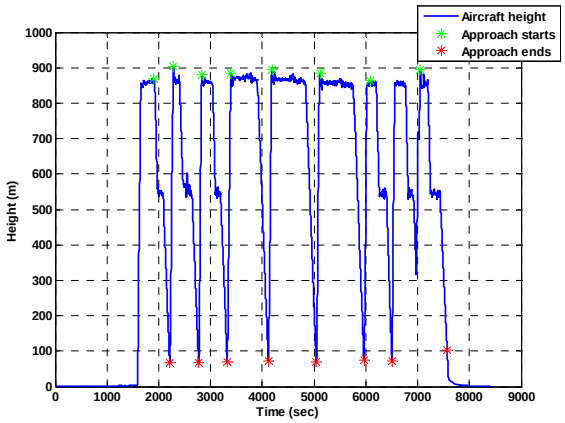

Fig 2: Flight Test Aircraft Altitudes

During each of the test approaches, the following data was collected and recorded:

Name	Remarks
GPS L1 data	GPS observation data
GPS L2 data	
GPS ephemeris	GPS navigation data
TSPI data	Aircraft positions
WAAS broadcast messages	

Table 1: Flight Test Data

Below illustrates the detailed contents in each of the data types:

1 Content of GPS observation data

Column	Data Name	Unit
1	GPS second	sec
2	PRN	/
3	Code measurements	m
4	Carrier smoothed code measurements	m
5	Smoothing time	sec
6	Carrier phase measurements	m
7	Time of carrier phase tracking at L1 frequency	sec
8	Time of carrier phase tracking at L2 frequency	sec
9	L1 frequency signal noise ratio	/
10	L2 frequency signal noise ratios	/
11	True ranges	m
12	WAAS fast corrections	m
13	WAAS clock corrections,	m
14	WAAS correction standard deviations	m

Table 2: Observation Data Content

2 TSPI data

This Time and Space Position Information data is generated with a GPS receiver and an IMU on the aircraft. The high-accuracy aircraft positions contained in this data file are considered to be the true reference positions in our data processing

3 WAAS Broadcast message

By receiving and decoding this message, the WAAS satellite ephemeris and clock corrections, also the ionosphere corrections will be produced.

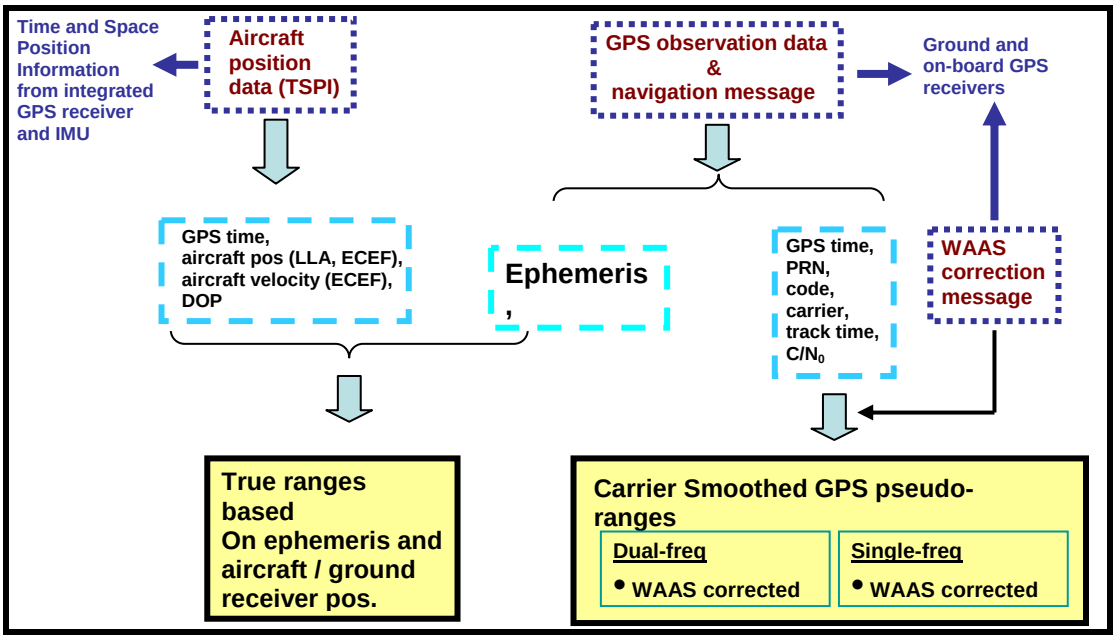

Fig 3: Flight Test Data Processing

The Flight test data processing procedures are shown in Figure 3. The WAAS correction messages are decoded and we apply the WAAS satellite ephemeris and clock corrections to the received GPS ephemeris so that the precise ephemeris is applied. From this precise is utilized. The WAAS troposphere correction model is applied to the received pseudorange, both L1 and dual-frequency, and the code measurements are smoothed with a 100-second carrier smoothing. For the L1 single-frequency pseudorange measurement, the WAAS ionosphere corrections are also applied.

Airborne Receiver Clock Error

The GPS code measurement error model is shown in Equation 6.

Single-frequency signal:

$$\rho_{air,L1} = r_{air} + B + eph + I_{L1} + T + b_{air} + \varepsilon_{air,L1}$$

Dual-frequency signal:

$$\rho_{air,DF} = r_{air} + B + eph + T + b_{air} + \varepsilon_{air,DF}$$

r_{air} : *Calculated range between the broadcast satellite position and the TSPI-derived precise aircraft position*

B : *Satellite clock error*

eph : *Satellite ephemeris error*

I : Satellite-receiver ionosphere delay

T : Satellite-receiver troposphere delay

b_{air} : *GPS receiver clock error*

ε_{air} : Multipath error and GPS receiver noise

Equation 6: GPS code measurement errors

The GPS code measurement error we inspected is basically the difference between the received pseudorange measurement and the calculated true range:

$$E = \rho_{air} - r_{air}$$

However, when we were checking the WAAS-corrected dual-frequency and single-frequency ephemeris and the TSPI-derived actual aircraft positions, the true reference pseudoranges will be formed and served as the standard for measuring the airborne GPS pseudorange quality. To generate the dual-frequency combined code measurement, Equation 4 code measurement errors, some unexpected results occurred when processing the flight test GPS measurement data with algorithms developed for static receiver data processing:

1. *There is only a small increase in the noise going from L1-only to Dual-freq signal*

-- Shown in Figure 4

2. *The carrier smoothing did NOT effectively reduce the apparent measurement noises*

-- Shown in Figure 5

Non-smoothed L1 code error distribution

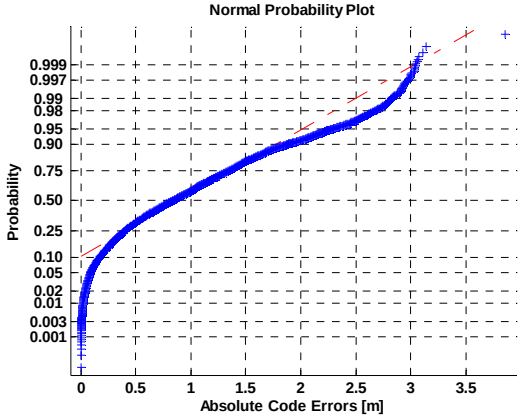

Non-smoothed dual-freq code error distribution

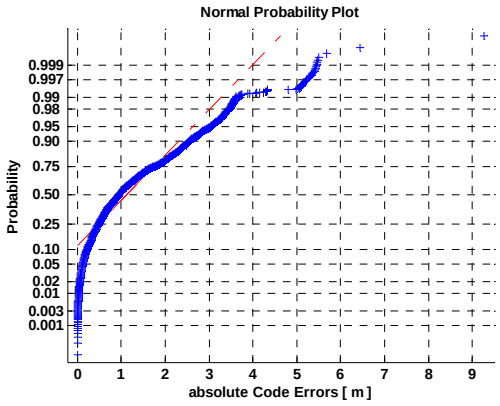

Fig 4: Small noise increase

Smoothed L1 code error distribution

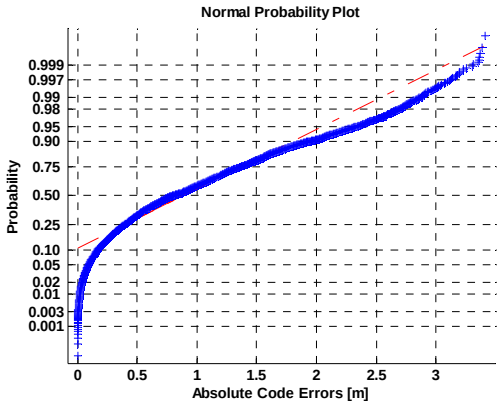

Smoothed dual-freq code error distribution

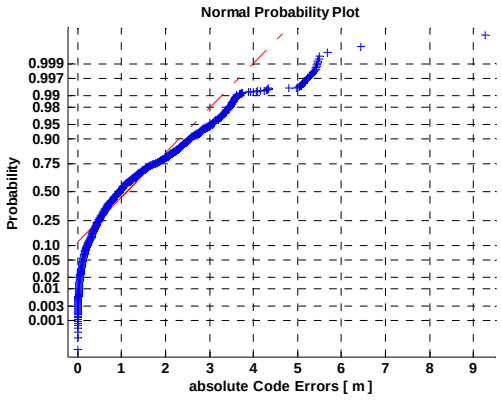

Fig 5: Carrier smoothing not reduce much noises

The error features we discovered with the airborne GPS code measurements are not consistent with those well established concepts:

- *Dual-freq signals should be much noisier than L1-only signals*

- *Carrier smoothing should effectively reduce code meas. Noises*

Therefore we realize there should be some unidentified error terms with these flight test GPS measurements. The code measurement errors of each of the individual satellites during one of the flight test approach are hereby investigated. From Figure 6, a dominant fast-changing error term exists across the ranging errors from each individual satellite (errors with other satellites are shown in Figure A1 in the appendix). Since it is identical across all satellites, this error term must

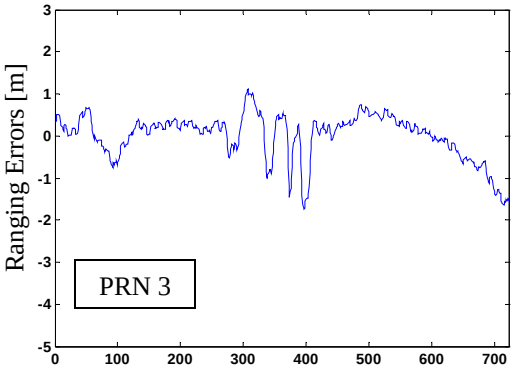

Fig 6. Ranging measurement error with individual satellite

be the airborne GPS receiver clock error. (Ranging errors with other satellites are shown in Appendix). And its variation rate and magnitude are much greater than ground receiver clock errors as we had processed previously (shown in Figure 7). Since the test aircraft was diving, climbing and maneuvering, the high rate and amplitude airborne GPS receiver error variation is believed caused by the acceleration and vibration of the test aircraft.

As the receiver clock error is the dominant error term, for us to clearly identify our desired ranging error characteristics, the receiver clock error needs to be estimated and excluded. From the error model in Equation 6:

$$\rho_{air,L1} = r_{air} + B + eph + I_{L1} + T + b_{air} + \varepsilon_{air,L1}$$

$$\rho_{air,DF} = r_{air} + B + eph + T + b_{air} + \varepsilon_{air,DF}$$

Since we have already applied the WAAS ephemeris corrections, clock corrections, troposphere corrections and ionosphere corrections (only to L1 signal), most of the ephemeris errors, satellite clock errors ionosphere errors (entire ionosphere errors for dual-frequency measurements) and troposphere errors have been eliminated, only small amount of residual errors remain. The equation 6 can be re-written as:

$$\rho_{air,L1} = r_{air} + b_{air} + \varepsilon_{air,L1} + \Delta e_{L1}$$

$$\rho_{air,DF} = r_{air} + b_{air} + \varepsilon_{air,DF} + \Delta e_{DF}$$

Equation 7: error model with corrections

Then the ranging errors are:

$$E_{air,L1} = \rho_{ai,L1} - r_{air} = b_{air} + \varepsilon_{air,L1} + \Delta e_{L1}$$
$$E_{air,DF} = \rho_{air,DF} - r_{air} = b_{air} + \varepsilon_{air,DF} + \Delta e_{DF}$$

Equation 8: remaining errors after corrections

After the WAAS corrections applied, the remaining errors are generally onboard receiver clock errors, multipath errors and receiver noise, also small amounts of residual errors (will be neglected in our process). As the multipath error and receiver noise are independent across different satellites and can be treated as noise, when we average the remaining errors from all satellite in view at a single time epoch, the average of the multipath errors and receiver noises is much reduced, and what we have will be the receiver clock error:

$$\frac{\sum E^{i}{}_{air,L1}}{n} = \frac{\sum b_{air}}{n} + \frac{\sum \varepsilon^{i}{}_{air,L1}}{n} + \Delta e \approx \frac{\sum b_{air}}{n} = b_{air}$$

$$\frac{\sum E^{i}{}_{air,DF}}{n} = \frac{\sum b_{air}}{n} + \frac{\sum \varepsilon^{i}{}_{air,DF}}{n} + \Delta e \approx \frac{\sum b_{air}}{n} = b_{air}$$

Equation 9: receiver clock error estimate

The airborne receiver clock error estimation result for one test approach is shown in Figure 7. The estimation of the ground receiver clock error is also plotted as a comparison.

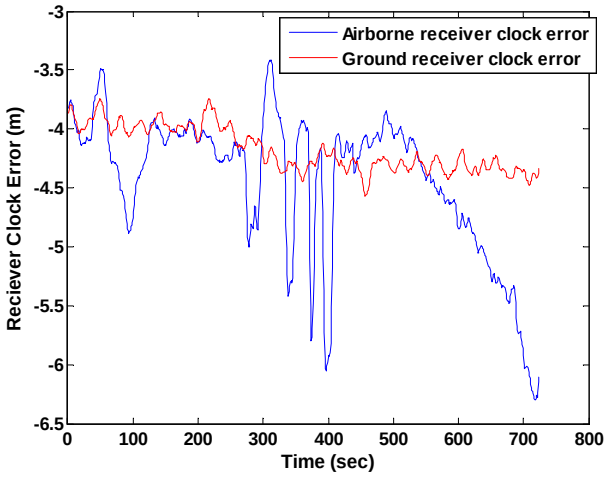

Fig 7: Receiver clock errors estimation result

Measurement noise and carrier smoothing

After estimating and excluding the GPS receiver clock error in the ranging measurements, we are able to investigate the desired error characteristics.

In Figure 8, after excluding the receiver clock errors, we inspected the WAAS-corrected pseudorange measurement errors before the carrier smoothing is applied. Therefore the main features shown in this figure will be the multipath error and receiver noise. It is clearly indicated that the measurement noise of the dual-frequency signal are much higher than the L1 signal, which agrees with the established theories.

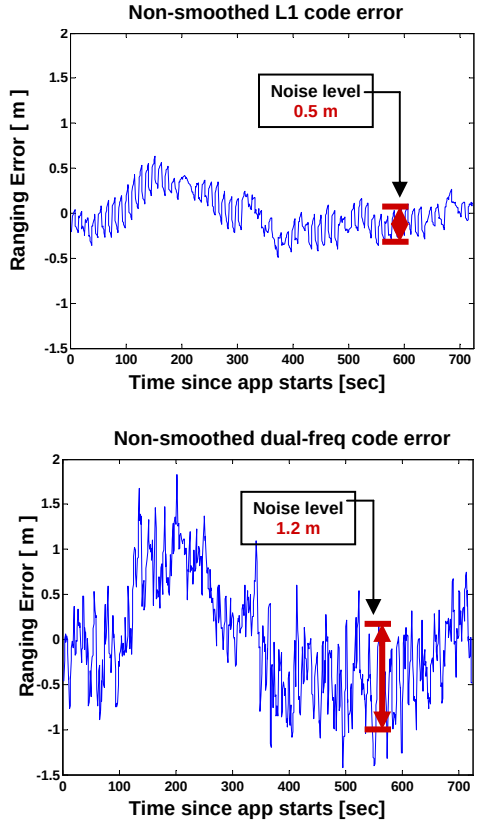

Fig 8: WAAS-corrected code meas. errors

After smoothing the code measurement with the 100-second carrier phase measurement, the dual-frequency signal noises dropped significantly as we expected (Figure 9).

However, there is still a low-frequency error (orange lines) remaining in the code measurement. This could be the residual error after the WAAS corrections or the error induced

by the receiver clock error estimation, which we will pay attention to it in our future work.

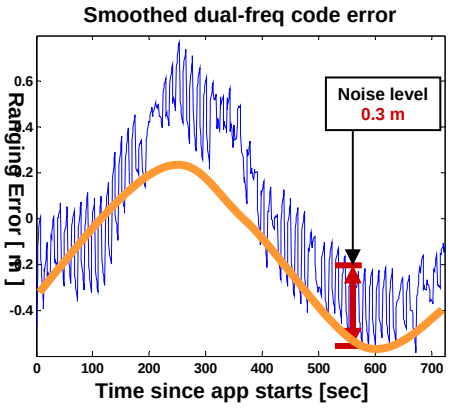

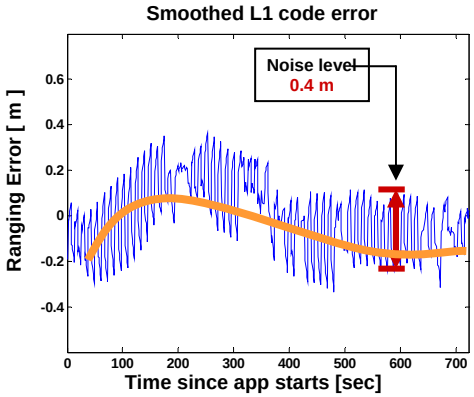

Statistical results also indicate that (shown in appendix Figure A2):

- *Dual-freq signals are noisier than L1-only signals*
- *Carrier smoothing effectively reduce code measurement Noises*

Conclusions

In the process of error characteristics validation with FAA flight test data, the high rate of on-board receiver clock variation makes identification of measurement errors more difficult. In this paper a receiver clock error estimation method is developed, which enables us to investigate the desired error characteristics. After mitigating the receiver clock error, the effectiveness of the carrier smoothing is validated by the flight test data, and we discovered two interesting error features:

- *The dual-frequency noise is less than 3 times of the L1-only noise, so the L2 noise is less than the L1 noise or there are still other effects exist*

- *Carrier smoothing works effectively so that the smoothed ranging error noises of both the L1 and dual-frequency signals are at a similar level.*

The future work will include more accurate receiver clock estimation technique to better reveal the desired error terms. Also with the more comprehensive understanding of the airborne GPS ranging measurement error features, the integrity model of GPS navigation application in civil aviation will be benefited.

Reference

[1] Misra, P., Enge, P., "Global Positioning System, Signals, Measurements and Performance", Page 162-169

[2] Klobuchar, J., "Ionospheric Effects on GPS", in "Global Positioning System: Theory and Applications, Vol. I, Parkinson, B., Spilker, J., Axelrad, P., and Enge, P.", AIAA

[3] RTCA, "Minimum Operational Performance Standards for GPS/WAAS Airborne Equipment", Dec 2006

Appendix

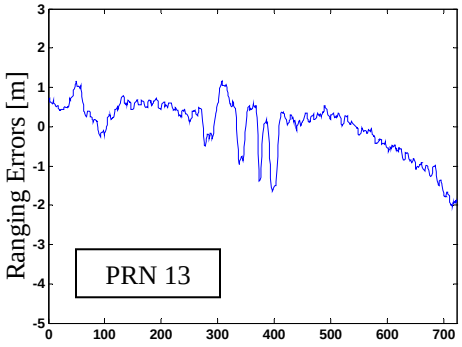

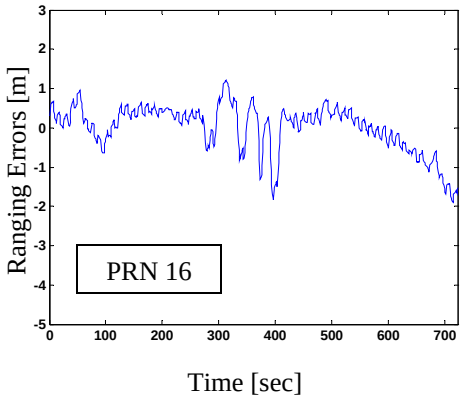

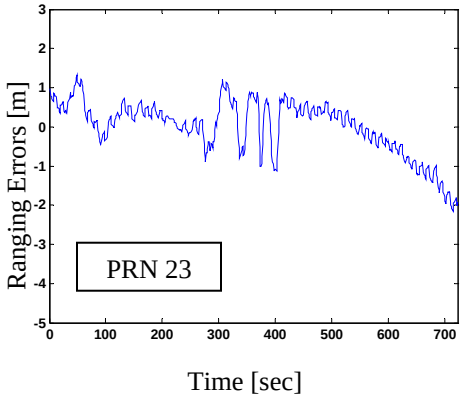

Fig A1: Ranging measurement error with individual satellite

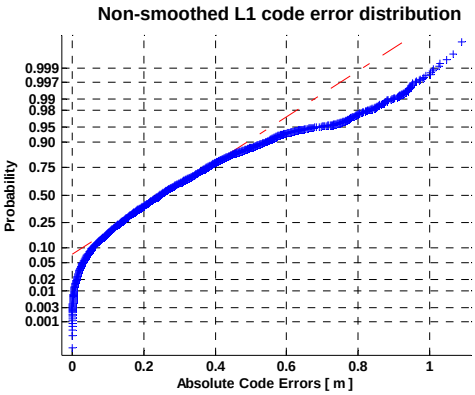

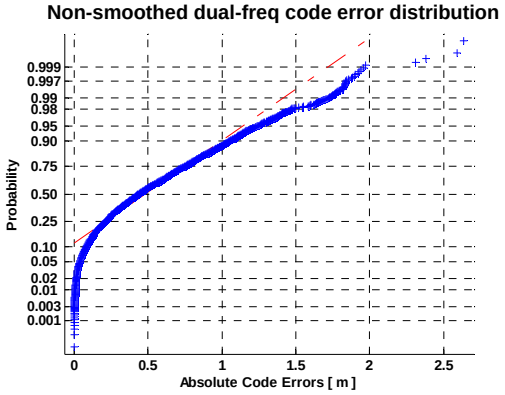

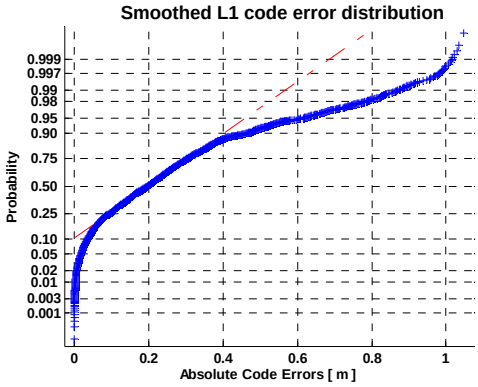

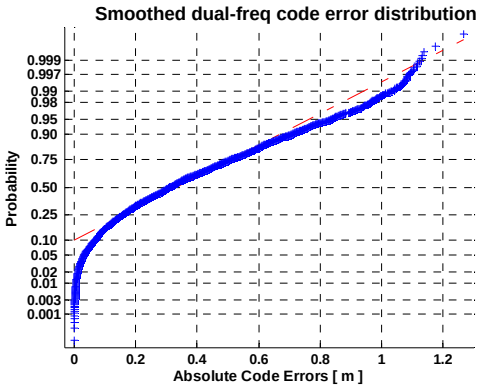

Fig A2: Measurement error result after excluding the airborne receiver clock bias